



Extended summary

Kinematic Boundary Layer Control on Airfoils for Wind Turbines in Free and Ducted Flows

Curriculum: Energy Sciences

Author

Enrico Renzi

Tutor

Ch.mo Prof. Renato Ricci

January 31st 2013

Abstract. The mathematical model of a wind turbine shows two different ways to increase the performance of the machine, i.e. modifying the stream tube around the turbine and/or the aerodynamic sections of the blade.

Placing the turbine in a diffuser or using a vortex behind the rotor section, the pressure drop and wind turbine performance increases. For every operating conditions the best performance can be obtained only if all the aerodynamic sections of the blade work properly.

A critical section is the blade root, where the operative conditions may induce the phenomenon of the local boundary layer separation named Laminar Separation Bubble (LSB). Airfoils, designed for the root section of a small wind turbine, were tested on the aeronautic wind tunnel of the “Università Politecnica delle Marche”.

In order to obtain a complete characterization of the LSB phenomenon and to evaluate the aerodynamic loads pressure measurements, wake analysis and infrared investigation were used. To reduce the LSB and increase the aerodynamic efficiency, mechanical disturbances inside the boundary layer were produced.

In the last part of the work a morphing wing section was designed and tested to evaluate the control of aerodynamic loads. This aspect is relevant especially for the new multi-megawatt wind turbines when the wind speed exceeds the nominal velocity.

Keywords. Laminar Separation Bubble (LSB), Morphing Wing, Shrouded Wind Turbine, IR Thermography

1 Introduction

The basic 1-D mathematical model of a wind turbine suppose that rotor is a permeable disk. This theory allows only to evaluate the force aligned with the flow direction, named thrust T (Hansen)[1].

Assuming that the mass of air passing through the disk remains separate from the air which does not cross the rotor section, a boundary surface can be drawn containing the air mass through the porous disk. This boundary can be extended upstream as well as downstream forming a stream-tube of circular cross section. (Burton)[2]. Close upstream of the rotor there is a small pressure rise from the atmospheric level, before a discontinuous pressure drop over the rotor. Downstream of the rotor the pressure recovers continuously to the atmospheric level. The pressure rising before and after the rotor section cause a continuous velocity decrease, therefore stream tube section increase in the flow direction in order to guarantee the mass continuity (Figure 1.1).

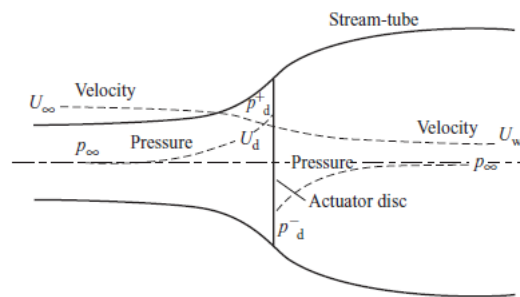


Figure 1.1: Pressure and velocity along the stream-tube

The rate of work done by the thrust force is $T \cdot U_d$ and hence the power extraction is given by:

$$P = T U_d = U_d A_d (p_d^+ - p_d^-) \quad 1.1$$

The dimensionless form of the power P is expressed as C_p , where P is divided by the available power P_{avail} for a cross section equal to the swept area A_d by the rotor,

$$P_{avail} = \frac{1}{2} \rho A_d U_d^3 \quad 1.2$$

$$C_p = \frac{P}{P_{avail}}$$

The classical 1-D momentum theory for free rotor, shows that maximum C_p value is 0.5926 named Betz limit.

Equation 1.1 shows that the extracted power and the C_p grow by increasing the pressure drop through the rotor section. By placing the rotor in a duct is possible to reduce the downstream pressure and exceed the Betz limit. There are two different way to obtain this effect, or placing the turbine in a diffuser or using a vortex behind the rotor section as show in Figure 1.2.

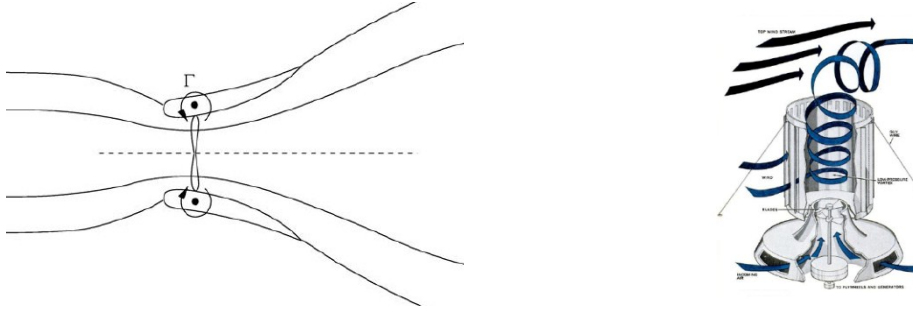


Figure 1.2: Shrouded wind turbine

If the cross-section of the diffuser is shaped like an airfoil (left Figure 1.2) , a lift force will be generated by the flow through the diffuser the effect of this lift force is to create a vortex ring, which induces a velocity component that increase the mass flow rate through the rotor (Hansen)[1].

In the turbine that using a vortex, named Tornado Type Wind Turbine (TTWT), the flow rate increase is due to a pressure drop in the core of the vortex respect the free stream (Yen)[3].

To study the interactions between flow and blade it is necessary to focalize the analysis on a single element of blade with a radial extension δr , using the Blade Element Momentum (BEM) theory (Burton)[2].BEM demonstrates that the tangential force δS produces the mechanical torque directly dependent to the airfoil efficiency ϵ defined as the ratio between lift on drag (C_l on C_d).

$$\delta S = \frac{N}{2} \rho V_{rel}^2 c \delta r C_l \sin \varphi \left(1 - \frac{1}{\epsilon \tan \varphi} \right) \quad 1.3$$

In the equation 1.3 N is the number of blades, φ is the angle between the relative velocity V_{rel} and the rotor plane and c is the blade element cord. The velocity incident V_{rel} on the airfoil is the composition of the wind velocity on the rotor section U_d and the peripheral velocity of the blade element.

The blade section with the lowest aerodynamic efficiency is localized on the root, caused by the lowest peripheral velocity hence the lowest relative velocity; moreover this section has the greatest thickness, needed to contain the structural element for the blade. These operative conditions may cause the phenomenon of the local boundary layer separation named Laminar Separation Bubble (LSB) (Eppler)[4] that induce a reduction of the aerodynamic efficiency.

We have to note that when the wind velocity grow beyond the nominal limit, the aerodynamic force produced by the blade it is extremely hence the mechanical safety may be compromised. In order to reduce the load on the rotor, it is possible modify the aerodynamic shape of the blade using a morphing wing that allow to moving the trailing edge.

2 Analysis and discussion of main results

To study the LSB and the morphing wing, three airfoils were build and tested in the aeronautic wind tunnel of the “Università Politecnica delle Marche”. The first two airfoils, named “RMR-3520” and “WT1”, were designed for the root sections of a small wind turbine; the third ,based on NACA 64,415, was built with a moving trailing edge.

For all the three wing sections a complete aerodynamic load characterization was made by pressure measurements and wake analyses, at following Reynolds number: 100000, 150000 and 200000. Were tested angles of attack α from -4° to 12° with step of 2° .

The “WT1” wing section was equipped with two different device that produce a surface vibration of the airfoil in order to reduce the extension of the LSB, the first one tested was a micro piezoelectric actuator, and the second one an unbalanced rotating mass. The vibration may reduce the laminar separation bubble when it is introduced in an unstable laminar boundary layer, this vibration was amplified to cause an anticipated turbulent transition (Schlichting)[5]. During the wing section building , pressure tabs were made in the middle section in order to measure the external pressure along the airfoil and calculate the lift force coefficient C_l produced and the aerodynamic moment at the aerodynamic centre $Cm_{c/4}$. To calculate the drag force coefficient C_d , wake analyses was made by used a rake of pitot that permits to evaluate the momentum losses due to the interaction between fluid and airfoil surface.

Also infrared investigations were used to localize the laminar separation bubble and evaluate the effect of the disturbance inserted in the boundary layer (Ricci) [6].

2.1 Analyses on RMR-3520

The first airfoil tested, built by using fiberglass, was the “RMR-3520” with a maximum thickness of 20% of the cord. In figure 2.1 is illustrated the dimensionless pressure coefficient c_p , where the almost constant zone in the upper surface indicates the presence of a laminar separation bubble. Figure 2.2 shows the velocity reduction in the wake region due to the momentum losses on the airfoil surface.

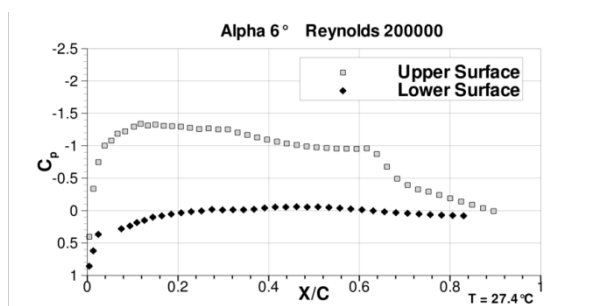


Figure 2.1: C_p at Reynolds 200000 and $\alpha 6^\circ$

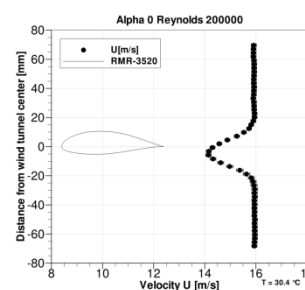


Figure 2.2: Wake analyses at Reynolds 200000 and $\alpha 0^\circ$

With c_p measurements was possible to calculate C_l and $Cm_{c/4}$ for all angle of attack, that combined whit wake analyses allow to plot the C_l C_d curve named Eiffel polar.

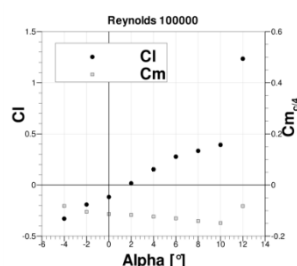


Figure 2.3: C_l , $Cm_{c/4}$ vs α at Reynolds 100000

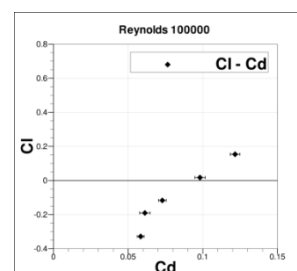


Figure 2.4: Eiffel polar at Reynolds 100000

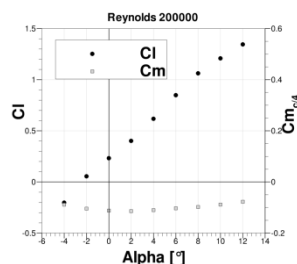


Figure 2.5: C_l , $C_{m_{c/4}}$ vs alpha at Reynolds 200000

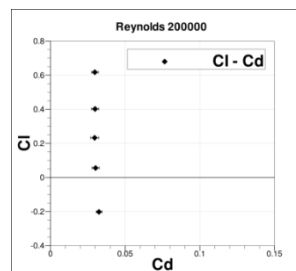


Figure 2.6: Eiffel polar at Reynolds 200000

Figure 2.3, and 2.4 show as at a lower Reynolds numbers the lift coefficient curve exhibits a non-linear behavior. Moreover the drag coefficient C_d is very high respect to the standard airfoils. At Reynolds number 200000 $C_l - \alpha$ curve exhibits a typical trend while the Eiffel polar with low and constant C_d value for the small angle of attack. The difference between the two Reynolds may due to an extended flow separation for the lowest one.

2.2 Analyses on WT1

This second airfoil, realized not in our laboratories, was built using 5 axis milling machine, was built with a cavity in the upper surface that allows to insert the vibrational device inside the wing section. The maximum thickness was again 20 % of cord, and for the lower Reynolds number the flow around the section was affected by long separated zone, as the RMR-3520. Tests at Reynolds number equal to 100000 whit both piezoelectric (Piezo) and unbalanced rotating mass (URM) show an important reduction of the LSB whit an increase of C_l and decrease of C_d that globally produce an improvement of the airfoil efficiency. External pressure measurements exhibit an high reduction of the almost constant zone in the c_p trend, while wake analyses shows an minor decelerate zone beyond the airfoil section. At Reynolds number 150000 this beneficial phenomenon is lesser.

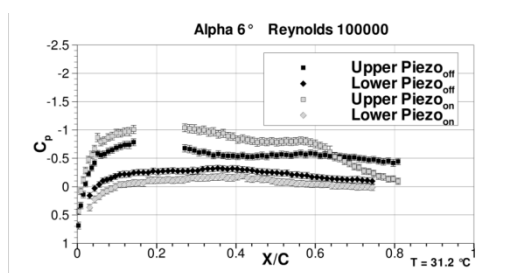


Figure 2.7: C_p whit and without the piezoelectric disturb at Reynolds 100000 an alpha 6°

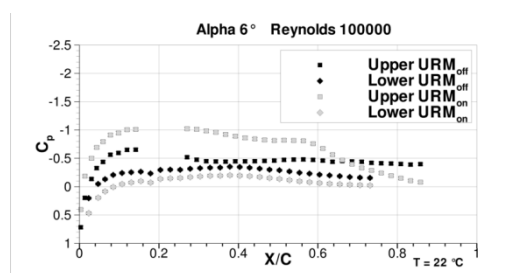


Figure 2.8: C_p whit and without the unbalanced mass disturb at Reynolds 100000 and alpha 6°

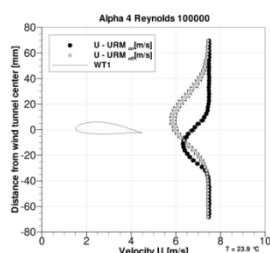


Figure 2.9: Wake analyses whit and without disturb at Reynolds 100000 and alpha 4°

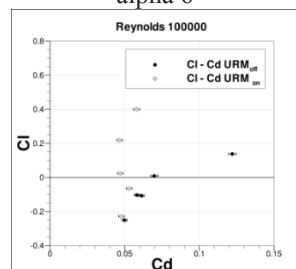


Figure 2.10: C_l , $C_{m_{c/4}}$ vs alpha whit and without disturb at Reynolds 100000

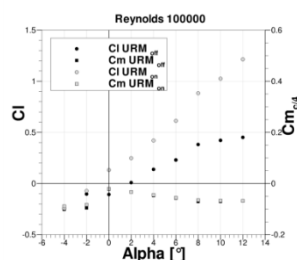


Figure 2.11: Eiffel polar whit and without disturb at Reynolds 100000

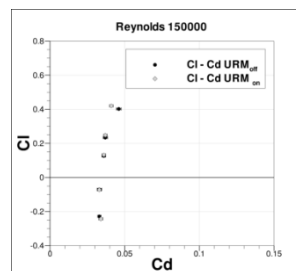


Figure 2.12: Eiffel polar whit and without disturb at Reynolds 150000

2.3 Infrared investigation on WT1

Covering the wing by a thin adhesive aluminum sheet and by using the Joule effect it was possible obtain a small increase of the airfoil surface temperature respect to the air. It is well known that laminar boundary layer shows a convective heat transfer coefficient h lesser than the turbulent boundary layer, thus in the turbulent zone a lesser temperature is obtained. The worse condition for the heat transfer it's the separated flows then in the zone of the laminar separation bubble the surface temperature shows the higher value. Measuring the surface temperature by the infrared machine model "Flir SC 3000" the contour of the surface temperature shows the presence of the LSB where the high temperature is located. To individuate the separation point of the laminar boundary layer, the transition point to a turbulent flow, and the turbulent reattachment point, the convective heat transfer coefficient h was calculated by a finite difference approach.

Figure 2.13, and 2.14 show the temperature contours and the convective coefficient on the WT1 at Reynolds number 100000 at alpha 6°. In figure 2.14 it is shown the case with piezoelectric disturbance, the lower extensions of the high temperature zone indicate an effective reduction on the laminar separation bubble. As the convective coefficient h , the dimensionless Stanton number was used to evaluate the local heat transfer, plotted in the same figures.

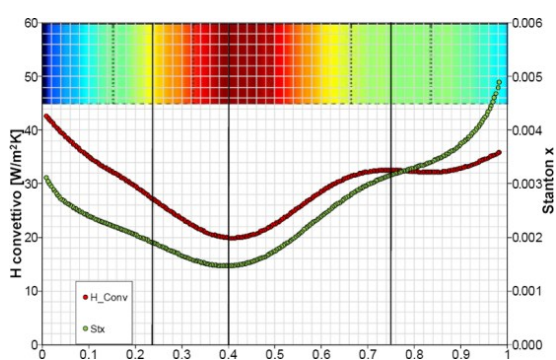


Figure 2.13: IR contours at Reynolds 100000 and alpha 6° without disturbance

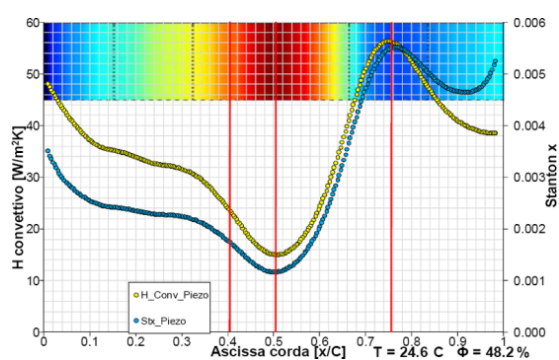


Figure 2.14: IR contours at Reynolds 100000 and alpha 6° with disturbance

2.4 Analyses on NACA64₂415 morphing wing

The third wing section was made in fiberglass and equipped by a moving trailing edge, actuated with a pulley designed and built in the “Università Politecnica delle Marche”. Figures 2.15 and 2.16 show the not-deformed shape and the maximum deformation respectively.

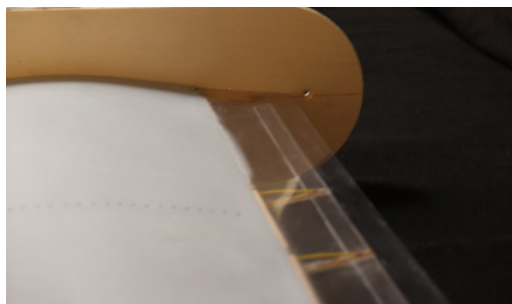


Figure 2.15: Not-deformed trailing edge

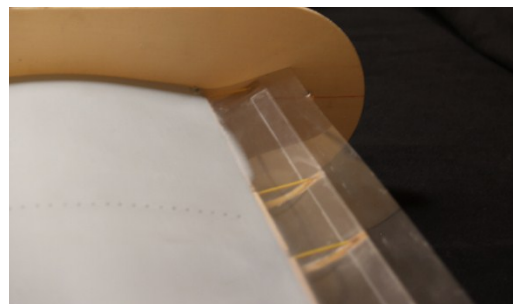


Figure 2.16: Maximum trailing edge deformation

Pressure measurements showed a reduction of the minimum pressure on the airfoil nose and the pressure distribution on the suction side tends to approach the pressure side one. Remembering that the lift coefficient is proportional to the area between the two curves, the increasing deformation produces a decreasing of the C_l due to the effective reduction of the maximum camber of the airfoil, and the angle of attack. Wake analyses shows a shifting of the decelerate zone in the direction of the trailing edge movement. At the low angle of attack tested for which the flow separation is smaller than the original shape, the wake of the deformed airfoils shows a deceleration zone larger than the not-deformed case.

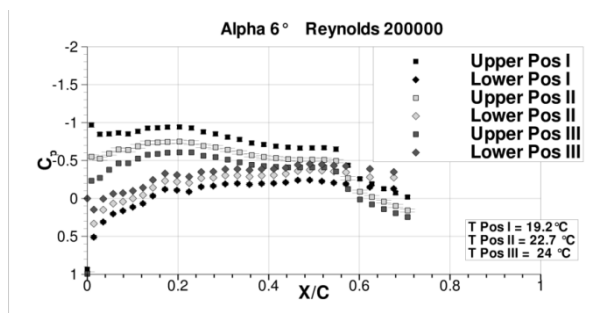


Figure 7.15: Pressure measurements for three different deformation at Reynolds 200000 alpha 6°

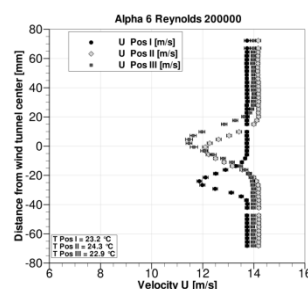


Figure 2.18: Wake analyses for three different deformation at Reynolds 200000 alpha 6°

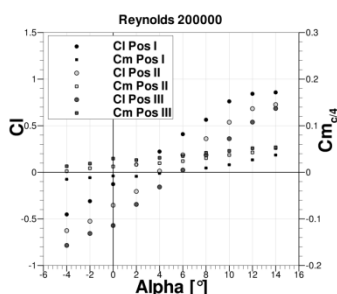


Figure 7.15: C_l , $C_{m_{c/4}}$ vs alpha at Reynolds 200000

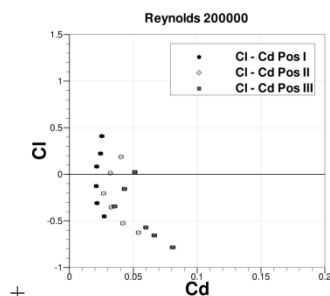


Figure 2.18: Eiffel polar at Reynolds 200000

In the above figures Pos I indicate the not-deformed shape while Pos III the maximum deformation. Extending the pressure analyses to $\alpha 14^\circ$ it was possible evaluate an effective stall delay. The Eiffel polar illustrate a C_d rise when the deformation increase.

3 Conclusions

Studies on various wing section have demonstrate that at low Reynolds numbers, the root section of a wind turbine blade are always affected by extended separation zone presenting the phenomena of laminar separation bubble.

With pressure measurements all around the airfoil and with infrared analyses it was possible to individuate the separated flow. By means of the introduction of a mechanical disturbance inside the laminar boundary layer before the separation point but after the minimum pressure, at the lower Reynolds number tested 100000, an important reduction of the laminar separation bubble was detected. The global effect of the disturbance is an increase of the lift coefficient, calculated by the pressure measurements, and a decrease of the drag coefficient, obtained from wake analyses, this means an increase of the efficiency for the wing section.

The morphing wing, realized starting by the NACA64₂415 shape, offers good performance in control of the aerodynamic forces. The lift force, evaluate whit external pressure measurements, decrease moving the trailing edge in the upper surface direction; the same measure permits also to calculate the aerodynamic moment at the aerodynamic centre, that is become positive for the deformed wing as a reflex airfoil. Wake analyses shown an increase drag deforming the trailing edge, but the analyses were related only at lowest angle of attack. Future work will be devoted to load cell balance measurement in order to permit the complete understanding the effect of the moving trailing edge.on the drag at highest angle of attack

References

- [1] Martin O. L. Hansen. *Aerodynamics of Wind Turbines*. EARTHSCAN, second edition, 2008.
- [2] Tony Burton, David Sharpe, Nick Jenkins, e Ervin Bossanyi. *Wind Energy Handbook*. John Wiley & Sons, 2001.
- [3] James T. Yen. *Investigation of the tornado wind energy system*. Technical report, Grunmman Aerospace Corp, Research and Development Center, 1982.
- [4] Richard Eppler. *Airfoil design and data*. Springer-Verlag, 1990.
- [5] Hermann Schlichting. *Boundary layer theory*. McGraw-Hill, seventh edition, 1979.
- [6] R. Ricci, S. Montelpare, e E. Renzi. Study of mechanical disturbances effects on the laminar separation bubble by means of infrared thermography. *International Journal of Thermal Sciences*, 2011.